Journal of Food Composition and Analysis 131 (2024) 106203

Contents lists available at ScienceDirect

Journal of Food Composition and Analysis

journal homepage: www.elsevier.com/locate/jfca

Towards an index of damage of olive paste during virgin olive oil extraction: The role of β-OH-acteoside diastereomers for risk assessment of the fusty/muddy sediment sensory defect

Lorenzo Cecchi [a], Carlotta Breschi [a,*], Lorenzo Guerrini [b], Silvia D'Agostino [a], Alessandro Parenti [a], Nadia Mulinacci [c], Bruno Zanoni [a]

[a] Department of Agriculture, Food, Environment and Forestry (DAGRI), University of Florence, Piazzale delle Cascine 18, Firenze, FI 50144, Italy
[b] Department of Land, Environment, Agriculture and Forestry (TESAF), University of Padova, Viale dell'Università 16, Legnaro, PD 35020, Italy
[c] Department of NEUROFARBA, Division of Pharmaceutical and Nutraceutical Sciences, University of Florence, Via U. Schiff 6, Sesto Fiorentino, FI, Italy

ARTICLE INFO

Keywords:
Kinetics modelling
malaxation
phenolic compounds
HS-SPME-GC-MS
panel test
volatile compounds
extra virgin olive oil
verbascoside

ABSTRACT

The aim of this study was to propose an index/marker of thermal/oxidative damage of olive paste during virgin olive oil extraction to assess the risk of sensory defects in the obtained oil. Several olive oil extraction trials were carried out over two production years applying different time, temperature, and oxygen exposure conditions during malaxation. The phenolic composition of the olive pastes was analyzed by High Performance Liquid Chromatography-Diode Array Detector-Mass Spectrometry (HPLC-DAD-MS). The chemical (legal quality indexes, phenolic compounds by HPLC-DAD-MS, volatile compounds by Head Space-Solid Phase Microextraction-Gas Chromatography-Mass Spectrometry (HS-SPME-GC-MS)) and sensory characteristics of the obtained oils were analyzed. The content of the β-OH-acteoside diastereomers in olive paste increased linearly with malaxation time as a function of malaxation temperature and oxidative conditions, following a pseudo-zero order kinetic. At the same time, two volatile compounds linked to sensory defects (2- and 3-methylbutanal) increased in the obtained oils when increasing malaxation time and temperature, and a relationship between them and the fusty/muddy sediment defect in olive oil samples was observed. A further direct relationship between the β-OH-acteoside content in the olive pastes and the 2+3-methylbutanal content in the oils was observed. Therefore, the β-OH-acteoside diastereomers content in olive pastes has been suggested as an index/marker to indicate the risk of sensory defects in virgin olive oil as a function of the thermal and oxidative conditions during malaxation. A threshold value of 100 mg/kg of the content of β-OH-acteoside diastereomers was proposed, above which the fusty/muddy sediment defect is perceptible.

1. Introduction

The constant challenge in food production processes is to achieve the required degree of the product characteristics while avoiding those collateral processing damages that can compromise safety, authenticity, nutritional value and sensory acceptability of foods and drinks, that is application of the so-called mild processing treatments (Abel et al., 2022; Rodgers, 2016). To this end, it is crucial to have indexes/markers related to known degradation phenomena to evaluate processing damage linked to these phenomena. Such indices should be able to show the effects of different operating conditions on processing damage in order to improve traceability and fraud detection in the food sector.

During processing, food products are subject to thermal and oxidative damages, often combined. Furosine and 5-hydroxymethyl-2-furfural (HMF) are the most common indexes/markers of thermal damage, since time and temperature of thermal processing have an

Abbreviations: ANOVA, Analysis of Variance; DAD, Diode Array Detector; EVOO, Extra virgin olive oil; HHS, high headspace; HMF, 5-hydroxymethyl-2-furfural; HPLC, High Performance Liquid Chromatography; HS-SPME-GC-MS, Head Space-Solid Phase Microextraction-Gas Chromatography-Mass Spectrometry; IOC, International Olive Council; LHS, low headspace; LOX, lipoxygenase; MISN, Multiple Internal Standard Normalization; MSD, Mass Spectrometry Detector; PCs, phenolic compounds; POD, peroxidases; PPO, polyphenol oxidases; VOO, virgin olive oil; VOC, Volatile Organic Compound.

* Corresponding author.
E-mail addresses: lo.cecchi@unifi.it (L. Cecchi), carlotta.breschi@unifi.it (C. Breschi), lorenzo.guerrini@unipd.it (L. Guerrini), silvia.dagostino@unifi.it (S. D'Agostino), alessandro.parenti@unifi.it (A. Parenti), nadia.mulinacci@unifi.it (N. Mulinacci), bruno.zanoni@unifi.it (B. Zanoni).

https://doi.org/10.1016/j.jfca.2024.106203
Received 3 November 2023; Received in revised form 19 February 2024; Accepted 21 March 2024
Available online 29 March 2024

important effect on the Maillard reaction (Giannetti et al., 2021; Nursten, 2005). All lipid-containing foods are susceptible to the well-known auto-oxidation and photo-oxidation reactions of triglycerides (Frankel, 1991). Plant materials are at risk of adverse changes during processing due to the oxidative damage of phenolic compounds and vitamins (Toydemir et al., 2022). The kinetic mechanisms of oxidative phenomena are complex and varied; therefore, a wide range of indexes/markers have been proposed, tailored on the involved material (Arnold and Gramza-Michalowska, 2022). They include the concentration of compounds resulting from the different steps of oxidative phenomena, colour indexes, enzymatic browning activity and antioxidant properties (the latter being measurable (Bocharova, 2022) by antioxidant/antiradical activity assays such as the Folin-Ciocalteu assay and the 2,2-diphenyl-1-picrylhydrazyl (DPPH) assay, and by electrochemical methods such as cyclic voltammetry and potential of platinum electrode).

Extra virgin olive oil (EVOO) is potentially subject to several thermal and oxidative damages occurring during extraction process, but also during storage and distribution (Cecchi et al., 2019; COI, 2018a; Guerrini et al., 2020). The unit operation of extraction by physical separation of the oil from the olive paste represents a break in the optimization of processing conditions: different phenomena occur before oil extraction, where the material is at high values of water activity (i.e., olives and olive paste), and after oil extraction, where the material is at low values of water activity (i.e., veiled oil and filtered oil). Triglycerides oxidation phenomena prevail during EVOO storage and distribution; therefore, processing treatments following oil extraction should be carried out in such a way as to avoiding risk factors such as light exposure, air exposure and high temperatures (Cecchi et al., 2019; Zanoni, 2014), in order to keep the values of oxidative damage indexes as low as possible (e.g., peroxide value, K_{232}, K_{270} and volatile molecular markers of rancidity). However, the univocal application of mild processing treatments before oil extraction is scientifically still under discussion. The operating conditions of olive milling and olive paste malaxation influence the kinetics of numerous biological, chemical, and physical phenomena, potentially causing both positive and negative effects on the quality of the extracted oil. Literature data shows that planning and control of olive paste malaxation require a complex balance between time, temperature, and oxygen level conditions: the values of these parameters can indeed be contradictory to each other when considering oil extraction yield, extraction of phenolic compounds and formation of volatile compounds by the lipoxygenase (LOX) pathway (Angerosa et al., 2001; Clodoveo, 2012; Trapani et al., 2017a; Trapani et al., 2017b). However, it is unquestionable that the unit operations before oil extraction should be carried out in suitable conditions to avoid the onset of oil sensory defects such as the fusty/muddy sediment defect, which is due to spoilage microbial activities leading to those volatile compounds related to such an off-flavour (Aparicio et al., 2012; Breschi et al., 2022; Cayuela et al., 2015; Cecchi et al., 2021a; Guerrini et al., 2019; Guerrini et al., 2020; Kalua et al., 2006). Consequently, it can be useful to measure the effects of operating conditions before oil extraction on olive paste by means of an index/marker of thermal and oxidative damage, which should also be able to predict the unwanted quality characteristics (i.e., sensory defects) of the obtained oil. Such an index/marker is still lacking up to now.

Verbascoside is one of the most abundant phenolic glycosides in olives after oleuropein (Cecchi et al., 2013; Ryan et al., 2002) but, due to its chemical structure bearing two sugar moieties, it is not extracted in virgin olive oil (VOO) (Klen and Vodopivec, 2012). Garcia-Rodriguez et al. (2011) showed that verbascoside was the best substrate for polyphenol oxidase having the largest number of hydroxyl groups in the benzene ring. A kinetic study of thermal and oxidative damage during malaxation of olive paste was carried out by Trapani et al. (2017b), working under high oxidative conditions at temperatures ranging from 22 to 37 °C. An increase in the content of β-OH-verbascoside diastereomers, also known as β-OH-acteoside diastereomers, occurred with time. It followed a pseudo-zero order kinetic, with rate constants which were temperature dependent through the Arrhenius equation. The β-OH-acteoside diastereomers were considered products of the verbascoside degradation due to a hydroxylation reaction. The above simple cause and effect relationship between olive paste treatments and β-OH-acteoside diastereomers content inspired the study presented in this manuscript.

The aim of the study was to evaluate the sensitivity of the β-OH-acteoside diastereomers content to changes in malaxation time and temperature under different oxidative conditions. The potential performance of the β-OH-acteoside diastereomers in risk assessment of the oil sensory defects was also studied for the first time.

2. Materials and methods

2.1. Olive samples

Homogeneous batches of approx. 80 kg of olive fruits (*Olea europaea* L., Frantoio cv) were picked from the same orchard (Fattoria Altomena, Florence, Italy) during the 2021 (25th October) and 2022 (7th November) olive oil production years. Each year, the batch was split into 2-kg aliquots, which were stored at 4 °C. This temperature did not allow the freezing of olives, thus avoiding the onset of the frostbitten olives defect and did allow hydrolytic phenomena to be minimized. The aliquots were then processed within 3 days of harvest (i.e., the shortest possible time) to obtain olive paste samples and olive oil samples, as described in Section 2.4.

2.2. Chemicals and standards

Ultrapure water from the Milli-Q-system (Millipore SA, Molsheim, France) was used for both extraction and HPLC analysis purposes. The following solvents and acids were used for HPLC analysis: acetonitrile with HPLC grade (Panreac, Barcelona, Spain); methanol with HPLC grade (Merck, Darmstadt, Germany); orthophosphoric acid (> 85%, Merck, Darmstadt, Germany). Other solvents used for extraction procedures were hexane, methanol, and ethanol with analytical grade (Merck, Darmstadt, Germany). Standards for analysis of phenolic compounds in olive paste and olive oil samples were tyrosol (> 99.5%, Merck, Darmstadt, Germany), *p*-coumaric acid (≥ 98%, Merck, Darmstadt, Germany), caffeic acid (≥ 98%, Merck, Darmstadt, Germany), verbascoside (> 99%, Extrasynthese, Genay, France), oleuropein (> 98%, Extrasynthese, Genay, France) and rutin (> 99% Extrasynthese, Genay, France); syringic acid (> 95%, Merck, Darmstadt, Germany) was used as the internal standard for analysis of phenolic compounds in olive oils. All internal and external standards (8 and 72 standards, respectively) used for HS-SPME-GC-MS analysis of volatile organic compounds (VOCs) of olive oil samples were from Merck (Darmstadt, Germany); the list and the purity of these standards can be found in Table S1. A refined olive oil free from interfering VOCs was used for preparing solutions of VOCs to be used for quantitation purpose according to the Multiple Internal Standard Normalization approach (MISN) approach (Cecchi et al., 2019).

2.3. Lab scale olive oil extraction plant

A lab-scale plant (Corti et al., 2023) was used for oil extraction. The plant consisted of a hammer mill with crushing holes with a 6-mm diameter (Mori TEM, Florence, Italy), a vertical axis malaxation equipment (Bagnoli David, Florence, Italy) and a centrifuge (NEYA 8xs, Remi Elektrotechnik Ltd., Palghar, India). The malaxer (Fig. S1A) consisted of a closed cylindrical jacketed tank (0.10 m internal diameter, 0.20 m height and 0.01 m jacket thickness) with a maximum capacity of approx. 1.2 kg of olive paste. It is equipped with a rotating shaft (43 rpm) with eight blades having a distance from the wall of less than 0.1 cm (Fig. S1B); the rotating shaft was installed on the top lid, and it was

powered by a 24 V electric motor (P205 24.64, Micro Motors, Lecco, Italy). The tank jacket was connected to both a refrigeration unit (CIL-LS037PA/404, Rivacold, Pesaro e Urbino, Italy) and a thermostatic bath (Kiss 205B, Huber, Offenburg, Germany), which provided cooling and heating of the process fluids (water), respectively. Two probe housings were provided to measure the temperature of the olive paste and the process fluid in the middle of the malaxator and in the jacket outlet pipe, respectively. The malaxer was designed to ensure a homogeneous temperature profile of olive paste, avoiding colder or warmer zones through a high heat exchange surface/volume ratio and effective mixing and scraping of the internal wall. Moreover, the malaxer was able to knead the olive paste under different levels of air exposure according to the filling of olive paste.

2.4. Experimental trials

The olive oil extraction trials were carried out during two consecutive production seasons: 2021 and 2022. The values of malaxation time and malaxation temperature were chosen among those typically adopted in oil mill. The experimental trials performed are described below and summarized in Table S2.

The 2021 experimental trials aimed to cause various levels of thermal damage to olive paste under low oxidative conditions. For each trial, 2 kg of olives were crushed, and approx. 1.2 kg of the olive paste obtained were malaxed, completely filling the malaxer (i.e., low headspace). Different malaxation time-temperature conditions were applied in the different trials, as follows. Five trials were carried out at 26 °C (that is lower than the 27 °C required for declaring the VOO as "cold extracted" (Reg EU 2104/2022)) and different malaxation times (i.e., 0, 15, 30, 45, 60 min). Six trials were carried out for 30 min (selected as typical malaxation time usually applied in the oil mills) at different malaxation temperatures (i.e., 18, 22, 26, 30, 34, 38 °C).

The 2022 experimental trials aimed to cause various levels of thermal damage to olive paste under both low and high oxidative conditions. For each trial, 2 kg of olives were crushed, and the olive paste obtained was malaxed as follows. Four trials were carried out at 26 °C and different malaxation times (i.e., 0, 20, 40, 60 min), completely filling the malaxer with approx. 1.2 kg of olive paste (i.e., low headspace). Four trials were carried out at 30 °C and different malaxation times (i.e., 0, 20, 40, 60 min), completely filling the malaxer with approx. 1.2 kg of olive paste (i.e., low headspace). Four trials were carried out at 26 °C and different malaxation times (i.e., 0, 20, 40, 60 minutes), half filling the malaxer with approx. 0.6 kg of olive paste (i.e., high headspace).

All trials were carried out in triplicate, in three different days (26th-28th October 2021 and 8th-10th November 2022, respectively). Each day a replicate of all trials was performed applying a completely randomized order, which was different for each day. The potential effect of olives storage on the experimental data was minimized by carrying out trials under all time-temperature malaxation conditions on each working day. All olive oil samples were obtained by centrifugation of olive paste samples for 10 min at 20 °C and 4500 rpm (2828 × g).

2.5. Analysis of phenolic compounds in olive paste

Immediately after malaxation, approx. 4 g of olive paste were weighted into a plastic centrifuge tube, and the extractive hydroalcoholic solution (35 mL) was added as soon as possible in order to stop any ongoing enzymatic reaction. The obtained mixture was stored at −20 °C over the days in which experimental trials were carried out, and until the following extraction procedure. Phenolic compounds were extracted twice with 35 mL of EtOH:H_2O = 80:20 v/v, homogenizing the mixture for 60 min. After each extraction cycle, the mixture was centrifuged (0 °C, 10 min, 1667 × g) and the supernatant was recovered. The final hydroalcoholic solution was defatted twice with hexane (50 mL) and evaporated under vacuum. The residue was re-dissolved in MeOH:H_2O = 50:50 v/v (8 mL), and the obtained mixture was centrifuged for 10 min at 20 °C and 13,148 × g. The supernatant was immediately used for HPLC analysis.

Phenolic extracts were analyzed with an HP1100 liquid chromatograph provided with autosampler, binary pump and column heater module, and coupled to DAD detector (Agilent, Palo Alto, USA). Phenols were separated in a Poroshell 120, EC-C18 column (150×3.0 mm, 2.7 μm ps; Agilent, Palo Alto, USA) working at 26 °C. The mobile phase (flow rate 0.4 mL/min) was constituted of acetonitrile (A) and H_2O (B, pH 3.2, formic acid) and the elution was performed using the following multistep linear gradient; solvent B varied 95%-60% in 40 min, remained at 60% for 5 min, varied 60%-0% in 5 min, remained at 0% for 3 min and finally returned to 95% in 2 min. Equilibration time, 10 min. Injection volume, 2 μL. Chromatograms were recorded at 240, 280 and 330 nm. Furtherly, LC-MS analysis was performed with an HP 1260 liquid chromatograph provided with DAD and MSD detectors, and with an API/electrospray interface (Agilent Technologies), by using the same HPLC method described above and the following ESI parameters: nebulizer pressure, 1811 Torr; drying gas flow and temperature, 12.0 L/min and 350 °C; capillary voltage, 3500 V. Acquisition in full spectrum scan (range 100–1200 Th) in negative ion mode with fragmentor voltage at 200 V.

Quantitative analysis was performed using calibration lines of tyrosol (linearity range 0–1.21 μg; R^2 0.9999) for tyrosol, hydroxytyrosol and their glucosides (after applying, for hydroxytyrosol and its glucosides, a corrective factor according to Bellumori et al. (2018)); verbascoside (0–1.96 μg, R^2 0.9996) for β-OH-acteoside isomers 1 and 2 and verbascoside; oleuropein (0–3.16 μg, R^2 0.9986) for oleuropein derivative; *p*-coumaric acid (0–1.52 μg, R^2 0.9994) for comselogoside; caffeic acid (0–1.57 μg, R^2 0.9998) for chlorogenic acid and cafselogoside; rutin (0–2.25 μg, R^2 1.0000) for rutin, luteolin-7-*O*-glucoside and luteolin.

2.6. Free acidity, peroxide value, and UV spectrophotometric indices in olive oils

The legal quality parameters such as free acidity (%), peroxide value (meq_{O2}/kg) and UV spectrophotometric indices (K_{232}, K_{270} and ΔK) of the olive oil samples were measured within 2 hours of oil extraction. These analyses were carried out according to the European Commission methods (Reg. UE 2105/2022).

2.7. HPLC-DAD analysis of phenolic compounds in olive oils

Analysis of phenolic compounds of olive oil samples was carried out according to the official International Olive Council (IOC) method (COI, 2022). Phenolic compounds were extracted from 2 g of oil sample with 6 mL of MeOH:H_2O 80:20 solution in the presence of syringic acid as internal standard. They were then separated using a C18 SphereClone ODS column (5 μm, 250 × 4.6 mm id; Phenomenex, Bologna, Italy), methanol, acetonitrile and water (acidified to pH 2.0 with H_3PO_4) as elution solvents and following the elution gradient (1 mL/min flow rate) described in the official method. The chromatograms were recorded at 280 nm. The quantitative analysis was carried out using syringic acid as internal standard and tyrosol as reference compound, therefore results were expressed as mg_{tyr}/kg.

Different methods were used for analysis of phenolic compounds in olive paste and olive oil because of the different nature of phenols present in virgin olive oil and in olive paste. The IOC official method was applied for the analysis of olive oils but, since it is not suitable for analysis of the phenolic compounds of olive paste, a different method was applied for these samples.

2.8. HS-SPME-GC-MS analysis of volatile organic compounds in olive oils

Analysis of 72 volatile organic compounds (VOCs) was carried out using HeadSpace-Solid Phase Micro Extraction coupled to Gas Chromatography-Mass Spectrometry (HS-SPME-GC-MS). Each VOC was

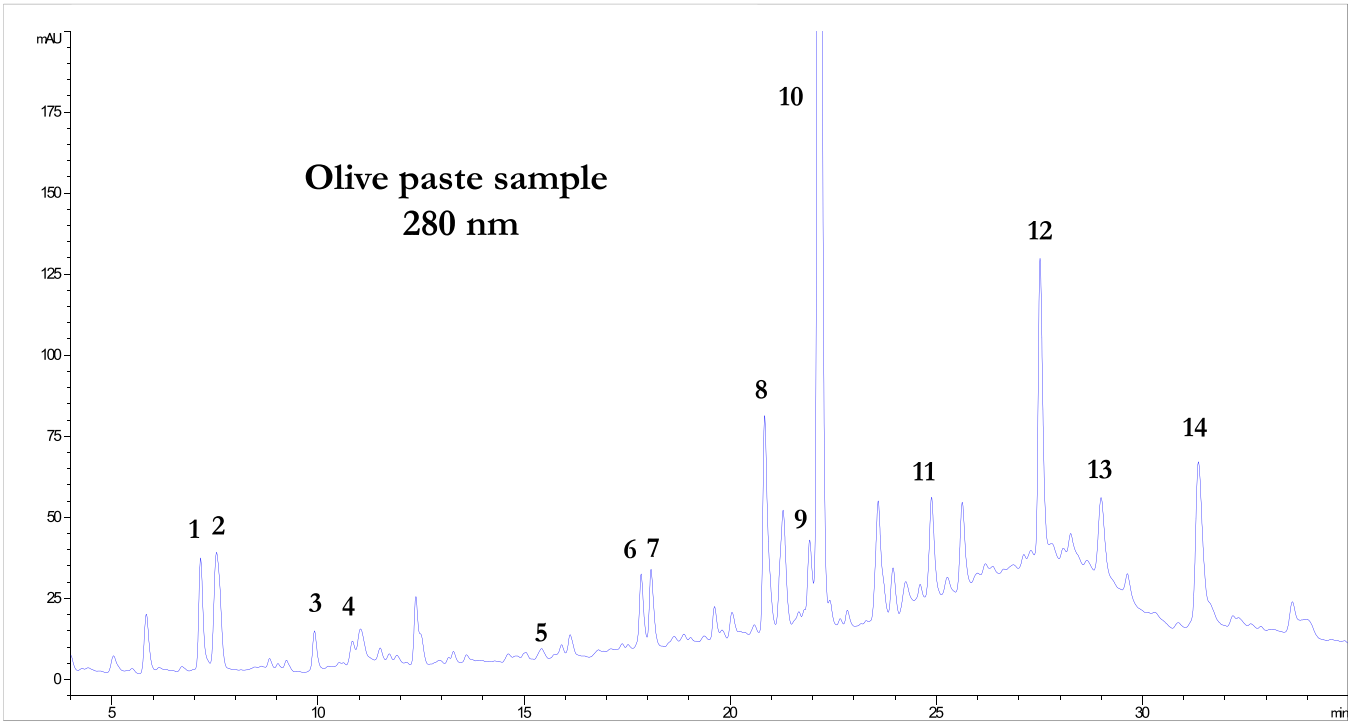

Fig. 1. Chromatographic profile at 280 nm of the 2022 olive paste sample at 26 °C, 60 min and High Headspace.*1, Hydroxytyrosol; 2, Hydroxytyrosol glucoside; 3, Tyrosol glucoside; 4, Tyrosol; 5, Chlorogenic acid; 6, β-OH acteoside isomer 1; 7, β-OH acteoside isomer 2; 8, Rutin; 9, Luteolin-7-O-glucosyde; 10, Verbascoside; 11, Caffeoyl-6-secologanoside (cafselogoside); 12, Oleuropein derivative; 13, p-coumaroyl-6'-secologanoside (comselogoside); 14, Luteolin.*

quantified using a previously validated method involving the MISN approach (Cecchi et al., 2019; Fortini et al., 2017). Briefly, 4.3 g of oil sample and 0.1 g of internal standards solution (in a refined olive oil free from interfering molecules) were added into a screw cap vial (20 mL). VOCs were pre-concentrated onto a 1-cm DVB/CAR/PDMS 50/30 μm SPME fiber (Agilent, Palo Alto, CA, USA), by exposing the fiber in the vial headspace for 20 min at 45 °C. After desorption (1.7 min at 260 °C) in the injection port of the 6890 N GC system, VOCs were separated with a HP-Innowax capillary column (50 m × 0.2 mm i.d., 0.4 μm film thickness), and detected using a 5975-model MS detector (Agilent, Palo Alto, CA, USA). Initial oven temperature was 40 °C for 2 min, then increased to 156 °C with a 4 °C/min flow, and to 260 °C with a 10 °C/min flow. Carrier gas: helium (1.2 mL/min). The transfer line and ion source temperatures were 250 °C and 230 °C, respectively. Mass detector worked in the *m/z* range of 30 – 350 Th (scan mode), 1500 Th/s, IE energy 70 eV. Seventy-two VOCs were identified by comparison with mass spectra and retention times of authentic standards. 2-Methylbutanol and 3-methylbutanol are co-eluting molecules; therefore, they were integrated together thus obtaining an output of 71 quantitative data for each sample. For each VOC, after selecting the most suitable internal standard for area normalization, a six-point linear least squares calibration line (plotting the area ratio against the amount ratio) was built using the relative pure standard and was used for quantitation purposes. For more details, the reader can refer to previous manuscripts concerning method set up and validation (Fortini et al., 2017; Cecchi et al., 2019).

2.9. Olive oil sensory analysis by Panel Test

The sensory attributes of olive oil sample were measured by a professional panel of ANAPOO (which are acknowledged by the Italian Ministry of Agricultural Policies (MIPAAF)) through the Panel Test method according to European Commission (Reg. UE 2105/2022; COI, 2018b). An aliquot of each olive oil sample was frozen at −20 °C immediately after extraction and thawed at room temperature immediately before tasting. Briefly, samples were presented to panelists in a randomized order and coded with three-digit number; the panelists were 8 tasters (trained according to the International Olive Council guidelines (COI, 2023)) coordinated by a panel leader. They smelt and tasted each olive oil and marked the intensity of negative (rancid, fusty/muddy sediment, musty/humid/earthy, winey/vinegary/acid/sour) and positive (fruity, pungent, bitter) attributes on a 0–10 cm unstructured scale, by using the profile sheet proposed by the method (COI, 2018b). Panelists rinsed their mouth with little slices of apple and water after tasting each sample. Four samples for session were tasted (COI, 2018b).

2.10. Statistical analysis

Experimental data were statistically processed according to Analysis of Variance (ANOVA) using Jamovi Statistical Software (JMP Statistical Discovery LLC). For the 2021 experimental trials, a one-way ANOVA was performed to assess: i) the effect of malaxation time at the same malaxation temperature; ii) the effect of malaxation temperature at the same malaxation time. For the 2022 experimental trials, a two-way ANOVA was performed to assess: i) the effect of malaxation time, oxidative conditions, and their interaction at the same malaxation temperature; ii) the effect of malaxation time, malaxation temperature and their interaction at the same oxidative conditions. Kinetic data of the β-OH-acteoside diastereomers and relationships between experimental data were processed using Table Curve 2D Version 4 software (Systos Software Inc., Richmond, CA).

3. Results and discussion

3.1. The β-OH-acteoside diastereomers and relevant formation kinetic models in the olive paste

A typical chromatogram at 280 nm of olive paste phenolic fraction is shown in Fig. 1, also including the list of the identified phenols.

Table 1
Effect of tested malaxation time (t), malaxation temperature (T) and oxidative conditions on the most important volatile compounds in olive oils and phenolic compounds in olive paste and in olive oils.

Compounds	2021		2022					
			HHS *vs* LHS trials at 26 °C			26 °C *vs* 30 °C trials at LHS		
	t at 26 °C	T at 30 min	t	HS	t × HS	t	T	t × T
	p-value	*p*-value	*p*-value	*p*-value	*p*-value	*p*-value	*p*-value	*p*-value
Verbascoside	n.s.	n.s.	*	n.s.	n.s.	n.s.	n.s.	n.s.
β-OH acteoside 1	*	n.s.	***	*	n.s.	**	n.s.	n.s.
β-OH acteoside 2	**	*	***	*	n.s.	**	n.s.	n.s.
Sum of β-OH diastereomers	**	n.s.	***	*	n.s.	**	n.s.	n.s.
Oleacein	***	***	***	n.s.	n.s.	***	n.s.	n.s.
Oleocanthal	***	***	***	n.s.	n.s.	***	n.s.	n.s.
Total phenols	***	***	*	n.s.	n.s.	*	n.s.	n.s.
Total LOX VOCs	n.s.	***	n.s.	n.s.	n.s.	n.s.	n.s.	*
Total "Rancid" VOCs	n.s.	***	**	**	n.s.	n.s.	***	n.s.
Total "Microbial" VOCs	***	*	***	n.s.	**	*	***	*
Sum of 2 and 3-methyl butanal	**	***	***	***	***	n.s.	***	***

***, p-value ≤ 0.001; **, p-value ≤ 0.01; *, p-value ≤ 0.05; n.s., not significant. HHS: high headspace. LHS: low headspace. 2021: experimental trials performed in the 2021 production year. 2022: experimental trials performed in the 2022 production year.

Table 2
β-OH-acteoside diastereomers and verbascoside contents (mean ± SD in mg/kg) in the olive paste samples (*OP*) depending on malaxation time-temperature and oxidative conditions.

2021 experimental trials

Compounds	OP at time zero	OP at 26°C −15 min - LHS	OP at 26°C −30 min - LHS	OP at 26°C −45 min - LHS	OP at 26°C −60 min - LHS	OP at 18°C −30 min - LHS	OP at 22°C −30 min - LHS	OP at 30°C −30 min - LHS	OP at 34°C −30 min - LHS	OP at 38°C −30 min - LHS
Verbascoside	1485 ± 87	1426 ± 110	1262 ± 122	1388 ± 133	1408 ± 164	1324 ± 40	1455 ± 179	1447 ± 188	1416 ± 214	1504 ± 144
β-OH acteoside 1	41.6 ± 3.5	43.5 ± 5.0	45.8 ± 1.8	50.9 ± 2.0	53.3 ± 4.5	44.8 ± 3.1	45.1 ± 2.9	48.2 ± 3.3	48.8 ± 3.9	51.1 ± 3.1
β-OH acteoside 2	42.3 ± 4.0	45.6 ± 4.9	52.0 ± 2.1	52.8 ± 4.9	58.7 ± 2.6	48.1 ± 2.9	49.0 ± 1.6	51.9 ± 2.1	53.1 ± 2.7	55.0 ± 2.3
Sum of β-OH diastereomers	83.9 ± 7.5	89.1 ± 9.4	97.8 ± 6.8	103.7 ± 6.8	112.0 ± 7.1	92.9 ± 9.2	94.1 ± 8.9	100.1 ± 10.6	101.9 ± 10.1	106.1 ± 10.9
Normalized sum of β-OH diastereomers	1	1.06	1.17	1.24	1.33	1.11	1.12	1.19	1.21	1.26

2022 experimental trials

Compounds	OP at time zero	OP at 26°C −20 min - HHS	OP at 26°C −40 min - HHS	OP at 26°C −60 min - HHS	OP at 26°C −20 min - LHS	OP at 26°C −40 min - LHS	OP at 26°C −60 min - LHS	OP at 30°C −20 min - LHS	OP at 30°C −40 min - LHS	OP at 30°C −60 min - LHS
Verbascoside	1410 ± 38	1521 ± 257	1621 ± 247	1427 ± 124	1515 ± 190	1653 ± 190	1460 ± 176	1533 ± 80	1496 ± 69	1560 ± 81
β-OH acteoside 1	63.2 ± 4.2	65.9 ± 3.9	78.1 ± 3.0	84.3 ± 1.5	66.3 ± 5.9	72.2 ± 5.3	74.0 ± 6.1	66.7 ± 4.5	73.2 ± 6.0	77.8 ± 2.5
β-OH acteoside 2	71.7 ± 2.5	73.8 ± 3.7	84.5 ± 3.5	89.0 ± 1.3	75.8 ± 5.5	76.8 ± 6.0	79.7 ± 5.7	74.6 ± 6.0	78.4 ± 6.2	86.1 ± 2.9
Sum of β-OH diastereomers	134.9 ± 5.2	139.7 ± 7.6	162.6 ± 6.1	173.3 ± 1.7	142.1 ± 11.3	149.0 ± 11.3	153.7 ± 10.9	141.3 ± 9.9	151.6 ± 11.8	163.9 ± 2.5
Normalized sum of β-OH diastereomers	1	1.04	1.21	1.28	1.05	1.10	1.14	1.05	1.12	1.21

HHS: high headspace. LHS: low headspace.

Secoiridoid derivatives, phenylpropanoids and flavonoids were the identified classes of phenolic compounds. In the 2021 olive paste samples, the phenylpropanoid verbascoside was by far the most abundant compound (1262–1504 mg/kg), followed by the oleuropein derivative and rutin (data not shown). In the 2022 olive paste samples, verbascoside was still the most abundant compound (1410–1653 mg/kg), followed by the oleuropein derivative, rutin and luteolin (data not shown). Overall, olive paste samples showed the greatest amounts of phenolic compounds in 2021; according to Cecchi et al. (2013), the 2021 olive samples could have had a lower ripening degree.

A significant behavior of β-OH-acteoside diastereomers was observed as a function of time-temperature and oxidative malaxation conditions (Table 1 and 2). Table 2 shows the content of each β-OH-acteoside diastereomer, their sum, their normalized sum (i.e., ratio between the sum of the β-OH-acteoside diastereomers contents and the sum at time zero) and the content of verbascoside in olive paste samples. The normalized sum of the β-OH-acteoside diastereomers (Δ_{rel}) increased linearly with malaxation time (t), and a pseudo-zero order kinetic was used to model the experimental data as follows:

$$\Delta_{rel} = 1 + kt \quad (1)$$

where k is the rate constant (1/min) as a function of temperature and oxidative conditions. This kinetic model confirmed the original kinetic model of the normalized sum of the β-OH-acteoside diastereomers by Trapani et al. (2017b), which was then used as the reference for the

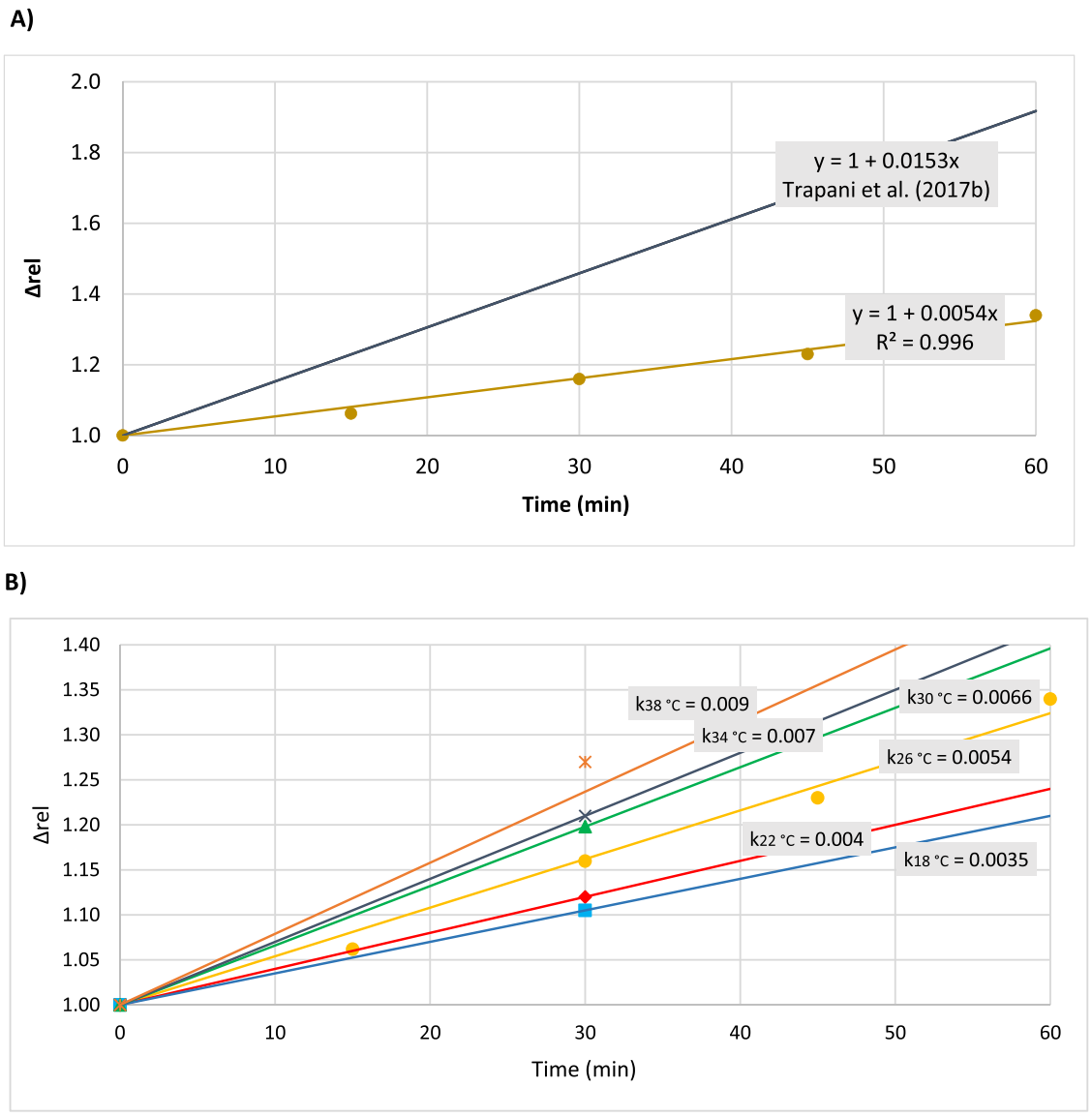

Fig. 2. A) Kinetics of Δ_{rel} (i.e., the normalized sum of the β-OH-acteoside diastereomers) at 26 °C: comparison between 2021 experimental data and Trapani et al. (2017b) data. B) Kinetics of Δ_{rel} at the different temperatures of 2021 experimental trials, assuming that the linear increase of Δ_{rel} occurred at all experimental malaxation temperatures.

following discussion.

During the 2021 experimental trials, a significant linear increase in Δ_{rel} with malaxation time was observed at 26 °C. It was approx. three times slower than the increase in Δ_{rel} at the same temperature as determined by the Trapani et al. (2017b) (Fig. 2A). Trapani et al. (2017b) studied malaxation under high oxidative conditions using the Abencor lab equipment, while low oxidative conditions were tested in the 2021 experimental trials of this study (i.e., complete filling of the lab closed vertical malaxer - Low Headspace/LHS), meaning that Δ_{rel} can be affected by air exposure, increasing more with increasing oxidative conditions. The Arrhenius approach was also applied to model the combined effect of time-temperature and oxidative conditions on the increase in Δ_{rel}, comparing the kinetic data by Trapani et al. (2017b) with the 2021 experimental data of this study. Assuming that the linear increase in Δ_{rel} occurred at all experimental malaxation temperatures of the 2021 trials, the related rate constants were determined (Fig. 2B), which were significantly temperature dependent through the Arrhenius equation as follows:

$$k = k_0 \exp\left(-\frac{E_a}{RT}\right) (\mathrm{R2} = 0.98;\ \mathrm{F} = 183) \quad [2]$$

where the frequency factor was $k_0 = 8230\ \mathrm{min}^{-1}$, the activation energy was $E_a = 35511$ J/mol, the gas constant was $R = 8.314$ J/(mol×K) and T was the absolute temperature (K). The lower Arrhenius constants from the kinetic data by Trapani et al. (2017b) (i.e., $k_0 = 6413\ \mathrm{min}^{-1}$, $E_a = 32184$ J/mol) can be explained by the high oxidative malaxation conditions, showing the oxidative origin of the formation of β-OH-acteoside diastereomers from verbascoside.

The 2022 experimental trials showed even more clearly the significant linear increase in Δ_{rel} with malaxation time as a function of malaxation temperature and oxidative conditions (Fig. 3A): the kinetic at 26 °C was slower than that at 30 °C, and the kinetic at 26 °C under high oxidative conditions (i.e., half filling of the lab closed vertical malaxer - High Headspace/HHS) was even faster than that at 30 °C under low oxidative conditions (i.e., complete filling of the lab closed vertical malaxer - Low Headspace/LHS). The comparison of the 2021 and 2022 kinetics with the kinetic data at 26 °C by Trapani et al. (2017b)

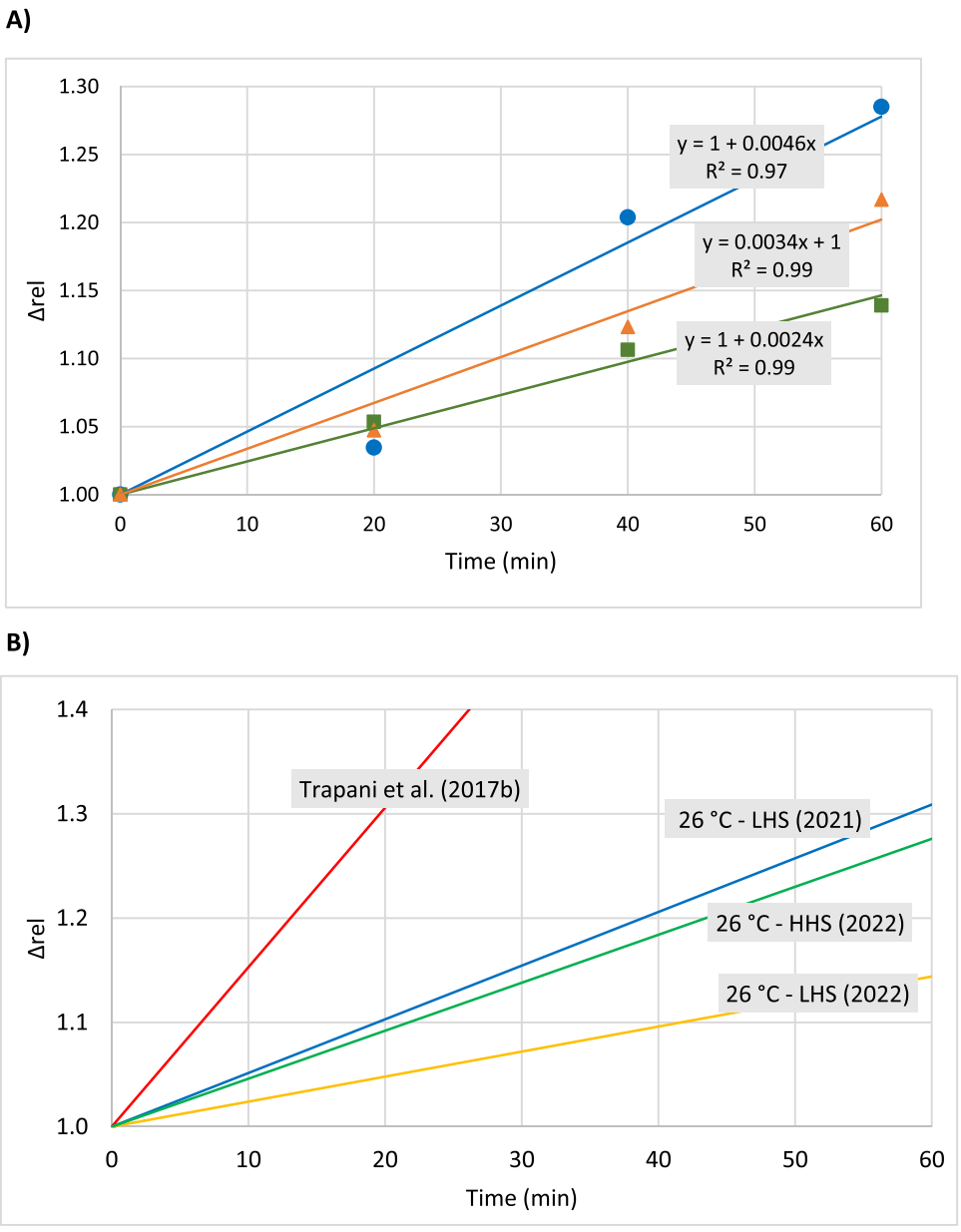

Fig. 3. A) Kinetics of Δ_{rel} (i.e., the normalized sum of the β-OH-acteoside diastereomers) at the different temperature and oxidative conditions in the 2022 experimental trials: ■ kinetic at 26 °C and low oxidative conditions (i.e., Low Headspace); ▲ kinetic at 30 °C and low oxidative conditions (i.e., Low Headspace); ● kinetic at 26 °C and high oxidative conditions (i.e., High Headspace). B) Comparison of the 2021 and 2022 kinetics with the kinetic data at 26 °C by Trapani et al. (2017b): (i) 26 °C – LHS (2022) = kinetic at 26 °C and low oxidative conditions in the 2022 trials (in orange); (ii) 26 °C – HHS (2022) = kinetic at 26 °C and high oxidative conditions in the 2022 trials (in green); (iii) 26 °C – LHS (2021) = kinetic at 26 °C and low oxidative conditions in the 2021 trials (in light blue); (iv) Trapani et al. (2017b) = kinetic at 26 °C and very high oxidative conditions according to Trapani et al. (2017b) (in red).

could also prove the effect of both the degree of oxidative impact and the olive quality on the kinetics of Δ_{rel} (Fig. 3B). The faster kinetic of Trapani et al. (2017b) could be caused by the combined effect of very high oxidative conditions due to the use of Abencor lab equipment (i.e., stainless steel mixing jars completely exposed to air) and a high aptitude of olives to the formation of the β-OH-acteoside diastereomers. This aptitude could similarly explain why the 2021 kinetic was faster than the 2022 kinetics.

The following phenomenological hypothesis of the formation of β-OH-acteoside diastereomers can be suggested from the discussed results. Scientific literature (Klen et al., 2015; Innocenti et al., 2006) suggests that β-OH-acteoside diastereomers differ from verbascoside for the presence of a hydroxyl group (-OH) on the -CH_2 directly linked to the phenolic ring on the hydroxytyrosol side of the molecule (Fig. S2). From the chemical reactivity viewpoint, hydroxylation in that position is quite unlikely, therefore it can be hypothesized that transformation of verbascoside into β-OH-acteoside is instead an oxidase enzymatic reaction (García-Rodríguez et al., 2011). The reaction leads to two diastereomers due to the generation of an additional stereogenic centre; therefore, the two new molecules have diverse chemical and chromatographic properties, and they are even separated in the chromatographic conditions usually applied for analysing the phenolic fraction of olive pastes (Fig. 1, peaks 6 and 7). The experimental data in Table 2 indicated similar amounts of the two diastereomers in all olive paste samples, suggesting a non-stereospecific nature of the enzymatic reaction. The chemical activities of polyphenol oxidases (PPO) and peroxidases (POD) are not able to explain the above hydroxylation reactions, since they usually oxidize a position of the phenolic ring and not an aliphatic carbon atom such as

Table 3
Phenolic compounds contents (mean ± SD in mg/kg) in olive oil samples (*OO*) obtained at different malaxation time-temperature and oxidative conditions.

2021 experimental trials										
Compounds	OO at time zero	OO at 26°C −15 min - LHS	OO at 26°C −30 min - LHS	OO at 26°C −45 min - LHS	OO at 26°C −60 min - LHS	OO at 18°C −30 min - LHS	OO at 22°C −30 min - LHS	OO at 30°C −30 min - LHS	OO at 34°C −30 min - LHS	OO at 38°C −30 min - LHS
Oleacein	109 ± 10	280 ± 69	318 ± 17	336 ± 22	352 ± 39	191 ± 33	260 ± 10	363 ± 43	421 ± 78	466 ± 68
Oleocanthal	80 ± 7	161 ± 33	188 ± 8	175 ± 18	183 ± 27	125 ± 27	154 ± 13	185 ± 3	207 ± 29	209 ± 36
Total phenols	799 ± 76	1021 ± 162	1158 ± 80	1078 ± 60	1120 ± 71	885 ± 71	1022 ± 29	1077 ± 112	1251 ± 171	1276 ± 174
2022 experimental trials										
Compounds	OO at time zero	OO at 26°C −20 min - HHS	OO at 26°C −40 min - HHS	OO at 26°C −60 min - HHS	OO at 26°C −20 min - LHS	OO at 26°C −40 min - LHS	OO at 26°C −60 min - LHS	OO at 30°C −20 min - LHS	OO at 30°C −40 min - LHS	OO at 30°C −60 min - LHS
Oleacein	90 ± 38	173 ± 17	189 ± 16	186 ± 16	179 ± 18	173 ± 30	173 ± 22	179 ± 36	238 ± 7	204 ± 20
Oleocanthal	69 ± 22	119 ± 5	132 ± 2	133 ± 4	119 ± 17	112 ± 24	114 ± 24	120 ± 14	146 ± 6	125 ± 12
Total phenols	460 ± 125	623 ± 61	653 ± 48	633 ± 63	596 ± 64	567 ± 89	561± 98	583 ± 79	726 ± 58	615 ± 59

HHS: high headspace. LHS: low headspace.

in the case of the transformation of verbascoside to β-OH-acteoside diastereomers (Nardella et al., 2023). Therefore, it is assumed that other oxidase enzymatic activities occurred, concerning the microbial contamination of the olive paste which, in turn, could explain the aptitude of olives to the formation of the β-OH-acteoside diastereomers as previously discussed (Angerosa et al., 1996; Zullo and Ciafardini, 2022).

3.2. *Effect of malaxation operating conditions on olive oil quality*

Free acidity, peroxide values, and UV spectrophotometric indices of the 2021 and 2022 olive oil samples are reported in Table S3: they were compliant with the EC regulation (Reg UE 2104/2022) for the EVOO commercial category. The experimental data did not show significant variations of these parameters as a function of time-temperature and oxidative conditions during malaxation. This is observation in agreement with the literature data (Cecchi et al., 2019; Cecchi et al., 2016), which mainly identify free acidity and oxidative indices (i.e., peroxide value, K_{232}, K_{270} and ΔK) with the degree of olives damage and oil storage conditions, respectively.

The PCs and VOCs contents, and the sensory attribute scores of the olive oil samples are reported in Tables 3, 4 and 5, respectively. Table 3 reports the total content of PCs and the content of the two secoiridoids usually most abundant in EVOO (Miho et al., 2020): oleacein (i.e., 3, 4-DHPEA-EDA) and oleocanthal (i.e., *p*-HPEA-EDA). Literature data (Nardella et al., 2023; Trapani et al., 2017b) suggest that phenolic compounds are subject to two opposite transformation phenomena during malaxation: (i) a decrease in phenolic compounds content due to oxidative phenomena caused by the activity of PPO and POX; (ii) an increase in phenolic compounds content due to phenomena such as mass transfer, enzymatic hydrolysis, and release of phenolic compounds from the cellular tissues. In the malaxation conditions of this research, the increasing phenomena prevailed over the enzymatic oxidative damage. The PCs content significantly changed with malaxation time and temperature (Table 1), increasing mainly from 0 min (i.e., no malaxation) to the minimum malaxation time (i.e., 15 min in the 2021; 20 min in the 2022): in particular, the total PCs content increased of approx. 40–60%, while oleacein and oleocanthal at least doubled their content (Table 3). Literature data also showed a similar behaviour (Nardella et al., 2023): for example, some manuscripts report a significant increase in oleacein and oleocanthal at increasing malaxation time in oils extracted working at different malaxations temperatures and oxidative conditions (Lukic et al., 2017; Lukic et al., 2018; Miho et al., 2020). The high scores for bitterness and pungency in the oil samples (Table 5) are in agreement with the known positive relationship between these sensory attributes and the PCs content in the EVOO (Andrewes et al., 2003; Gutiérrez-Rosales et al., 2003). The lower PCs content in the 2022 oil samples is consistent with the lower scores for bitterness and pungency.

VOCs were studied as groups of compounds usually associated with positive or negative sensory attributes of EVOO (Table 4). The VOCs originating from the LOX pathway (LOX VOCs) are reported in Table 4 as total content, as percentage of (*E*)-2-hexenal (i.e., the molecule associated with fruity notes (Cecchi et al., 2021b)), and as percentage of the different chemical classes. In all olive oil samples, (*E*)-2-hexenal was by far the most abundant compound, being approx. 85% of the total content of LOX compounds. The greatest contents of total LOX VOCs were found in the 2021 olive oil samples extracted at low malaxation temperatures: in fact, in the oils from the trials carried out at 18 and 22 °C for 30 min of malaxation, the total LOX VOCs content was significantly greater (approx. 1.5-fold) than that of the oils from the trials carried out at 26, 30, 34 and 38 °C for 30 min (Table 1). The optimal working temperature of the enzyme hydroperoxide lyase (i.e., 15 °C (Nardella et al., 2023)) can explain the above phenomenon, leading to an increase in LOX aldehyde compounds at lower malaxation temperatures. The scores for the fruity attribute of the oil samples (Table 5) are in agreement with the known direct relationship between this sensory attribute and the LOX VOCs content in the EVOO (Cecchi et al., 2021b). The lower LOX VOCs content in the 2022 oil samples is consistent with the lower score for fruity.

The VOCs associated with EVOO sensory defects were studied according to literature data as follows (Table 4): (i) the VOCs responsible for the rancid defect (Cecchi et al., 2019; Morales et al., 2005); (ii) the VOCs responsible for sensory defects due to the spoilage microorganisms (Cecchi et al., 2021a; Vichi et al., 2009; Zhu et al., 2016; Angerosa, 2002) and, among them, (iii) the content of the sum of 2- and 3-methylbutanal (which are responsible for the fusty/muddy sediment attribute) and their percentage on the total VOCs from spoilage microorganisms (Guerrini et al., 2020; Lukic et al., 2017; Cevik et al., 2016; Angerosa et al., 2001; Angerosa et al., 1996). The most interesting behavior was observed for the content of 2- and 3-methylbutanal (Table 1): in fact, their percentage content on the total "microbial" VOCs ranged between approx. 30 and 70%, and their content significantly increased as the malaxation times and temperatures increased. The effect of olives quality on this behavior can also be supposed. The olive oil samples obtained by working at 0 minutes of malaxation during the 2022 trials showed a content of the sum of 2- and 3-methylbutanal greater than that

Table 4
Volatile organic compounds contents (mean ± SD in mg/kg) in olive oil samples (*OO*) obtained at different malaxation time-temperature and oxidative conditions.

2021 experimental trials

Trial	LOX VOCs (%) Total LOX VOCs1 (mg/kg)	Esters	Alcohols	(E)-2-hexenal	Other aldehydes	Ketones	Total "Rancid" VOCs2 (mg/kg)	Total "Microbial" VOCs3 (mg/kg)	Sum of 2 and 3-methyl butanal (mg/kg)	Sum of 2 and 3-methyl butanal4 (%)
OO time zero	34.0 ± 4.9	2.62	4.63	87.00	3.77	1.97	0.609 ± 0.206	0.031 ± 0.003	0.012 ± 0.004	37.9
OO at 26 °C - 15 min - LHS	29.0 ± 2.9	3.61	5.76	84.35	3.92	2.37	0.523 ± 0.057	0.046 ± 0.011	0.023 ± 0.009	49.7
OO at 26 °C −30 min - LHS	29.6 ± 3.2	2.77	5.97	84.82	4.00	2.43	0.489 ± 0.003	0.042 ± 0.001	0.025 ± 0.002	60.9
OO at 26 °C −45 min - LHS	27.3 ± 4.9	3.75	6.11	84.01	3.95	2.18	0.468 ± 0.105	0.062 ± 0.009	0.042 ± 0.011	67.9
OO at 26 °C −60 min - LHS	24.2 ± 3.7	3.49	6.54	83.38	4.17	2.41	0.441 ± 0.085	0.075 ± 0.016	0.054 ± 0.017	71.4
OO at 18 °C −30 min - LHS	49.2 ± 5.0	1.52	4.41	87.76	3.96	2.35	0.812 ± 0.116	0.051 ± 0.006	0.014 ± 0.005	26.8
OO at 22 °C −30 min - LHS	40.6 ± 3.3	1.93	5.07	86.45	4.25	2.30	0.822 ± 0.058	0.048 ± 0.008	0.019 ± 0.006	38.2
OO at 30 °C −30 min - LHS	24.7 ± 2.2	3.90	6.30	83.31	4.05	2.45	0.476 ± 0.103	0.057 ± 0.003	0.034 ± 0.004	59.8
OO at 34 °C −30 min - LHS	23.6 ± 2.1	4.47	6.25	83.38	3.80	2.10	0.524 ± 0.061	0.067 ± 0.006	0.041 ± 0.008	60.3
OO at 38 °C −30 min - LHS	22.3 ± 1.8	4.52	6.44	83.21	3.91	1.92	0.594 ± 0.114	0.072 ± 0.009	0.051 ± 0.011	70.2

2022 experimental trials

Trial	LOX VOCs (%) Total LOX VOCs[1] (mg/kg)	Esters	Alcohols	(*E*)-2-hexenal	Other aldehydes	Ketones	Total "Rancid" VOCs[2] (mg/kg)	Total "Microbial" VOCs[3] (mg/kg)	Sum of 2 and 3-methyl butanal (mg/kg)	Sum of 2 and 3-methyl butanal (%)[4]
OO at time zero	20.7 ± 0.4	1.79%	5.82%	86.47%	3.49%	2.43%	0.150 ± 0.014	0.153 ± 0.021	0.074 ± 0.009	48.7
OO at 26°C - 20 min HHS	21.4 ± 2.0	1.82%	6.23%	86.13%	3.32%	2.49%	0.124 ± 0.013	0.297 ± 0.052	0.097 ± 0.012	33.0
OO at 26°C - 40 min HHS	20.4 ± 2.4	1.61%	6.84%	85.32%	3.49%	2.75%	0.149 ± 0.018	0.436 ± 0.035	0.146 ± 0.020	33.5
OO at 26°C - 60 min HHS	22.0 ± 2.3	1.54%	6.41%	85.86%	3.38%	2.81%	0.211 ± 0.015	0.318 ± 0.015	0.205 ± 0.016	64.5
OO at 26°C - 20 min LHS	19.7 ± 1.8	1.91%	6.34%	85.51%	3.66%	2.58%	0.177 ± 0.004	0.266 ± 0.020	0.090 ± 0.011	33.8
OO at 26°C −40 min LHS	23.5 ± 1.3	1.79%	7.24%	83.98%	4.50%	2.48%	0.171 ± 0.003	0.320 ± 0.030	0.126 ± 0.013	39.5
OO at 26°C −60 min LHS	21.8 ± 1.4	1.61%	7.47%	83.81%	3.97%	3.14%	0.255 ± 0.032	0.413 ± 0.032	0.174 ± 0.021	42.0
OO at 30°C −20 min LHS	20.7 ± 1.0	1.73%	6.26%	85.94%	3.35%	2.72%	0.222 ± 0.023	0.261 ± 0.008	0.100 ± 0.015	38.3
OO at 30°C −40 min LHS	19.9 ± 2.5	1.91%	6.37%	85.91%	3.41%	2.39%	0.205 ± 0.012	0.430 ± 0.040	0.120 ± 0.010	27.9
OO at 30°C −60 min LHS	21.8 ± 0.3	1.92%	6.56%	85.24%	4.05%	2.24%	0.252 ± 0.001	0.399 ± 0.021	0.213 ± 0.030	53.1

[1] Total LOX VOCs: sum of esters (hexyl acetate, (*Z*)-3-hexenyl acetate, (*E*)-2-hexenyl acetate), alcohols (1-hexanol, (*Z*)-3-hexenol, (*E*)-2-hexenol, (*E*)-2-pentenol, (*Z*)-2-pentenol, 1-penten-3-ol), ketones (1-penten-3-one), (*E*)-2-hexenal and other aldehydes (hexanal, (*Z*)-3-hexenal, (*E*)-2-pentenal)
[2] Total "rancid" VOCs: sum of pentenal, (*E*)-2-heptenal, nonanal
[3] Total "microbial" VOCs: sum of acetic acid, ethyl acetate, 2-methyl butanal, 3-methyl butanal, 1-octen-3-ol, 1-octen-3-one, 6-methyl-5-hepten-2-one
[4] Sum of 2 and 3-methyl butanal (%): percentage of the sum of 2 and 3-methyl butanal on the total microbial VOCs
HHS: high headspace. LHS: low headspace.

Table 5
Sensory attributes of the olive oil samples obtained at different malaxation time-temperature and oxidative conditions.

2021 experimental trials							
Trial	Fusty/muddy sediment	Musty/Humid/earthy	Winey/vinegary/acid/sour	Rancid	Fruity	Bitter	Pungent
OO at time zero	0	0	0	0	4	5	6
OO at 26°C −15 min - LHS	0	0	0	0	5	8	8
OO at 26°C −30 min - LHS	0	0	0	0	5	6	7
OO at 26°C −45 min - LHS	1	0	0	0	5	6	6
OO at 26°C −60 min - LHS	2	1	0	1	4	5	5
OO at 18°C −30 min - LHS	0	0	0	0	5	5	7
OO at 22°C −30 min - LHS	0	0	0	0	6	8	7
OO at 30°C −30 min - LHS	1	0	0	0	4	7	7
OO at 34°C −30 min - LHS	1	0	0	0	5	5	6
OO at 38°C −30 min - LHS	1	0	0	0	5	5	5
2022 experimental trials							
Trials	Fusty/muddy sediment	Musty/Humid/earthy	Winey/vinegary/acid/sour	Rancid	Fruity	Bitter	Pungent
OO at time zero	1	0	0	2	2	4	4
OO at 26°C −20 min - HHS	3	0	0	1	2	4	6
OO at 26°C −40 min - HHS	3	1	1	1	1	4	4
OO at 26°C −60 min - HHS	2	0	1	1	2	4	4
OO at 26°C −20 min - LHS	3	0	1	1	2	4	5
OO at 26°C −40 min - LHS	2	0	0	1	2	5	5
OO at 26°C −60 min - LHS	2	0	0	2	2	5	6
OO at 30°C −20 min - LHS	3	0	1	2	2	4	6
OO at 30°C −40 min - LHS	2	0	0	1	2	4	5
OO at 30°C −60 min - LHS	3	0	1	2	2	4	5

OO: olive oil. HHS: High Headspace. LHS: Low Headspace.

of all 2021 olive oil samples (i.e., 0.074 vs 0.012 mg/kg); on the opposite, the 2022 olive oil samples showed a slower increase in 2- and 3-methylbutanal content during malaxation than that of the 2021 olive oil samples. For example, when malaxation was carried out at 26 °C, 60 min and LHS, a 2.5- and 4.5-fold increase in 2- and 3-methylbutanal content was observed in olive oil samples from 2022 and 2021, respectively, compared to the trials carried out at 0 min of malaxation. The relationship described in the literature between the content of 2- and 3-methylbutanal and the fusty/muddy sediment defect in olive oil samples (Guerrini et al., 2020; Lukic et al., 2017; Cevik et al., 2016; Angerosa et al., 2001; Angerosa et al., 1996) may be observed (Table 5), and the 2022 oil samples were already defective for this sensory defect at time zero of malaxation.

3.3. Relationship between the β-OH-acteoside diastereomers and the 2- and 3-methylbutanal contents

The results of this research suggest original behaviors of the β-OH-acteoside diastereomers (*βOH*) and the 2- and 3-methylbutanal (*2,3But*) as a function of malaxation time, temperature, and oxidative conditions. Therefore, a relationship between their contents expressed in mg/kg was studied, obtaining the significant proportional trend according to the following equation (Fig. 4A):

$$[2,3But] = 0.002 \bullet [\beta OH] - 0.174 (R2 = 0.89;\ F = 170) \quad [3]$$

The phenomenological meaning of this relationship is not easy to explain based on the experimental data. It was assumed that amino acids metabolism of the spoilage microorganisms in the olive paste during malaxation caused the 2- and 3-methylbutanal formation (Dickinson et al., 2003), and that microbial growth was made possible by oxidase enzymatic activities (Sharma et al., 2016; Angerosa et al., 1996), including those relating to the formation of β-OH-acteoside diastereomers. The different behavior between the 2021 and 2022 samples may be consistent with this hypothesis: different kinetics of biological phenomena were pointed out in relation to the microbial quality of olive fruits, but the linear relationship in Eq. 3 has not been rejected.

Furthermore, the relationship reported in the literature between the fusty/muddy sediment defect and the 2- and 3-methylbutanal content (Guerrini et al., 2020; Lukic et al., 2017; Cevik et al., 2016; Angerosa et al., 2001; Angerosa et al., 1996) has been confirmed by the data of this research. Therefore, the β-OH-acteoside diastereomers content can be proposed as an index of the quality of olive paste for risk assessment of the fusty/muddy sediment defect as a function of the thermal and oxidative conditions of malaxation. In the experimental conditions of this research (Tables 4 and 5), the appearance of the fusty/muddy sediment defect in virgin olive oil samples occurred when the content of 2- and 3-methylbutanal reached approx. 0.04 mg/kg, which is related to a content of 105 mg/kg of the β-OH-acteoside diastereomers by the equation [3]. Therefore, a threshold value of 100 mg/kg of the content of β-OH-acteoside diastereomers can be suggested, above which a perceptible fusty/muddy sediment defect occur (Fig. 4B).

4. Conclusions

The content of the β-OH-acteoside diastereomers in olive paste was proposed as an original index for the risk assessment of the fusty/muddy sediment defect in virgin olive oil as a function of the thermal and oxidative conditions during oil extraction process. These compounds derive from verbascoside through enzymatic hydroxylation reactions and their trouble-free identification and quantification is carried out by HPLC-DAD analysis at 280 nm. Their content was sensitive to both time-temperature and oxidative conditions during malaxation according to simple pseudo-zero order kinetics, whose rate constant was temperature dependent via the Arrhenius equation. Based on the relationships between the contents of β-OH-acteoside diastereomers in olive paste and of 2- and 3-methylbutanal in the obtained oils, and the onset of the fusty/muddy sediment sensory defect, a threshold value of approx. A content of 100 mg/kg of β-OH-acteoside diastereomers in olive paste is proposed in order to predict a perceptible fusty/muddy sediment defect in the obtained oils (and the consequent non-conformities with European legal requirements for the EVOO category). Knowing the β-OH-acteoside diastereomers content after olives crushing and their formation kinetics

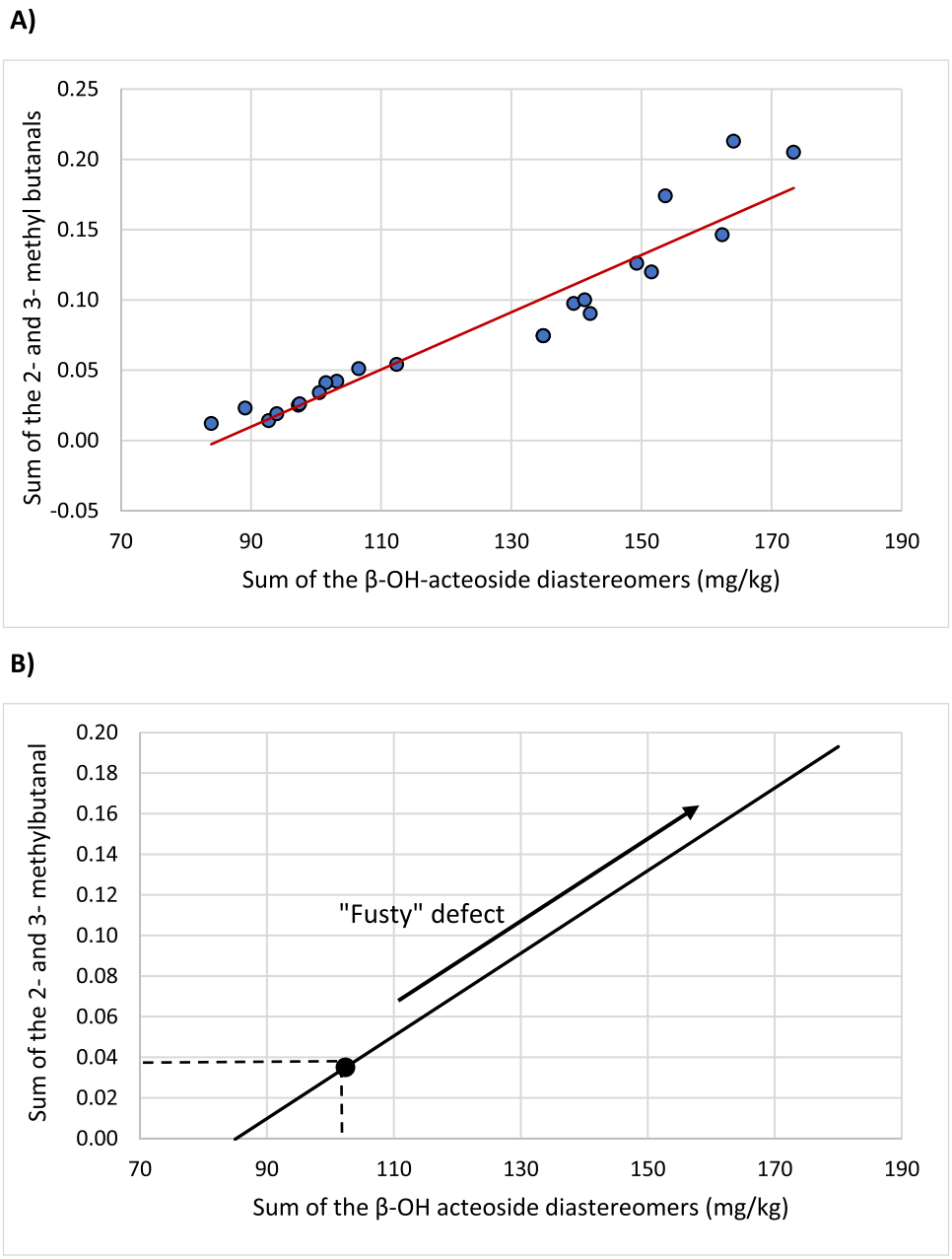

Fig. 4. A) Relationship between the content of the sum of β-OH-acteoside diastereomers and the sum of 2- and 3-methylbutanal. B) Suggested threshold value of the sum of β-OH-acteoside diastereomers content in olive paste above which an oil perceptible fusty/muddy sediment defect by panel test can occur.

can allow both assessing the risk of defects in oils to be extracted and applying the appropriate corrections to the malaxation process to facilitate extraction of phenolic compounds and/or formation of LOX VOCs also avoiding thermal and oxidative damage. Further investigations should be carried out to study the possible role of spoilage microorganisms on the β-OH-acteoside diastereomers formation, as hypothesized in this study.

Funding

This study was carried out within the Agritech National Research Center and received funding from the European Union Next-GenerationEU (PIANO NAZIONALE DI RIPRESA E RESILIENZA (PNRR) – MISSIONE 4 COMPONENTE 2, INVESTIMENTO 1.4 – D.D. 1032 17/06/2022, CN00000022). This manuscript reflects only the authors' views and opinions, neither the European Union nor the European Commission can be considered responsible for them.

CRediT authorship contribution statement

Lorenzo Guerrini: Methodology, Conceptualization. **Silvia D'Agostino:** Formal analysis, Data curation. **Alessandro Parenti:** Investigation, Data curation. **Nadia Mulinacci:** Methodology, Investigation. **Lorenzo Cecchi:** Writing – original draft, Methodology, Investigation, Formal analysis, Data curation, Conceptualization. **Carlotta Breschi:** Writing – original draft, Formal analysis, Data curation. **Bruno Zanoni:** Writing – original draft, Supervision, Project administration, Methodology, Funding acquisition, Conceptualization.

Declaration of Competing Interest

The authors declare that they have no known competing financial

interests or personal relationships that could have appeared to influence the work reported in this paper.

Data availability

Data will be made available on request.

Acknowledgements

Authors thanks to Prof. Piernicola Masella and Dr. Ferdinando Corti for the contribution in developing and using the lab scale plant, Nico Sartori (Fattoria Altomena, Pelago, Firenze, Italy) for providing olives, Claudia Ghinassi and Edoardo Meacci for helping during their thesis.

Consent for publication

All authors have reviewed and approved the final version of the manuscript for publication.

Appendix A. Supporting information

Supplementary data associated with this article can be found in the online version at doi:10.1016/j.jfca.2024.106203.

References

Abel, N., Rotabakk, B.T., Lerfall, J., 2022. Mild processing of seafood – A review. Compr. Rev. Food Sci. Food Saf. 21, 340–370. https://doi.org/10.1111/1541-4337.12876.

Andrewes, P., Busch, J.L.H.C., De Joode, T., Groenewegen, A., Alexandre, H., 2003. Sensory properties of virgin olive oil polyphenols: identification of deacetoxyligstroside aglycon as a key contributor to pungency. J. Agric. Food Chem. 51, 1415–1420. https://doi.org/10.1021/jf026042j.

Angerosa, F., Lanza, B., Marsilio, V., 1996. Biogenesis of "fusty" defect in virgin olive oils. Grasas Aceites 47 (3), 142–150. https://doi.org/10.3989/gya.1996.v47.i3.854.

Angerosa, F., Mostallino, R., Basti, C., Vito, R., 2001. Influence of malaxation temperature and time on the quality of virgin olive oils. Food Chem. 72 (1), 19–28. https://doi.org/10.1016/S0308-8146(00)00194-1.

Angerosa, F., 2002. Influence of volatile compounds on virgin olive oil quality evaluated by analytical approaches and sensor panels. Eur. J. Lipid Sci. Technol. 104, 639–660. https://doi.org/10.1002/1438-9312(200210)104:9/10<639::AID-EJLT639>3.0.CO;2-U.

Aparicio, R., Morales, M.T., Garcia-Gonzalez, D.L., 2012. Towards new analysis of aroma and volatiles to understand sensory perception of olive oil. Eur. J. Lipid Sci. Technol. 114, 1114–1125. https://doi.org/10.1002/ejlt.201200193.

Arnold, M., Gramza-Michalowska, A., 2022. Enzymatic browning in apple products and its inhibition treatment: a comprehensive review. Compr. Rev. Food Sci. Food Saf. 21, 5038–5076. https://doi.org/10.1111/1541-4337.13059.

Bellumori, M., Cecchi, L., Romani, A., Mulinacci, N., Innocenti, M., 2018. Recovery and stability over time of phenolic fractions by an industrial filtration system of olive mill wastewaters: a three-year study. J. Sci. Food Agric. 98 (7), 2761–2769. https://doi.org/10.1002/jsfa.8772.

Bocharova, O.V., 2022. Electrochemical basis for re-evaluating antioxidant effect of redox substances in foodstuffs. ACS Food Sci. Technol. 2, 738–750. https://doi.org/10.1021/acsfoodscitech.2c00002.

Breschi, C., Guerrini, L., Parenti, A., Masella, P., Calamai, L., Lunetti, L., Zanoni, B., 2022. Turbidity characterization as a decision-making tool for extra virgin olive oil stability treatments. Food Control 137, 108931. https://doi.org/10.1016/j.foodcont.2022.108931.

Cayuela, J.A., Gomez-Coca, R.B., Moreda, W., Perez-Camino, M.C., 2015. Sensory defects of virgin olive oil from a microbiological perspective. Trends Food Sci. Technol. 43 (2), 227–235. https://doi.org/10.1016/j.tifs.2015.02.007.

Cecchi, L., Migliorini, M., Cherubini, C., Giusti, M., Zanoni, B., Innocenti, M., Mulinacci, N., 2013. Phenolic profiles, oil amount and sugar content during olive ripening of three typical Tuscan cultivars to detect the best harvesting time for oil production. Food Res. Int. 54, 1876–1884. https://doi.org/10.1016/j.foodres.2013.04.033.

Cecchi, L., Migliorini, M., Cherubini, C., Trapani, S., Zanoni, B., 2016. The case of the 2014 crop season in Tuscany: a survey of the effect of the olive fruit fly attack. Ital. J. Food Sci. 28, 352–361.

Cecchi, L., Migliorini, M., Giambanelli, E., Rossetti, A., Cane, A., Mulinacci, N., 2019. New volatile molecular markers of rancidity in virgin olive oils under nonaccelerated oxidative storage conditions. J. Agric. Food Chem. 67, 13150–13163. https://doi.org/10.1021/acs.jafc.9b05809.

Cecchi, L., Migliorini, M., Giambanelli, E., Cane, A., Mulinacci, N., Zanoni, B., 2021a. Volatile profile of two-phase olive pomace (Alperujo) by HS-SPME-GC-MS as a key to defining volatile markers of sensory defects caused by biological phenomena in virgin olive oil. J. Agric. Food Chem. 69 (17), 5155–5166. https://doi.org/10.1021/acs.jafc.1c01157.

Cecchi, L., Migliorini, M., Mulinacci, N., 2021b. Virgin olive oil volatile compounds: composition, sensory characteristics, analytical approaches, quality control, and authentication. J. Agric. Food Chem. 69 (7), 2013–2040. https://doi.org/10.1021/acs.jafc.0c07744.

Clodoveo, M.L., 2012. Malaxation: influence on virgin olive oil quality. Past, present and future – An overview. Trends Food Sci. Technol. 25 (1), 13–23. https://doi.org/10.1016/j.tifs.2011.11.004.

COI. (2018a). Best practice guidelines for the storage of olive oils and olive-pomace oils. COI/BPS/Doc. No 1. https://www.internationaloliveoil.org/wp-content/uploads/2019/11/COI-BPS-Doc.-No-1-2018-Eng.pdf (latest access, 24th June, 2023).

COI. (2018b). Sensory analysis of olive oil. Method for the organoleptic assessment of virgin olive oil. COI/T.20/Doc. No.15/Rev. 10. https://www.internationaloliveoil.org/wp-content/uploads/2019/11/COI-T20-Doc.-15-REV-10-2018-Eng.pdf (latest access, 21th April, 2023).

COI. (2022). Document to declare the use of IOC methods for phenolic compounds determination. COI/T.20/Doc. No.29/Rev. 2. Method 1. Determination of biophenols in olive oils by HPLC. COI/T.20/Doc. No.29/Rev. 1 2017. https://www.internationaloliveoil.org/wp-content/uploads/2022/06/Doc.-No-29-REV-2_ENK.pdf (latest access, 29th May, 2023).

COI. (2023). Guide for the selection, training and quality control of virgin olive oil tasters – qualifications of tasters, panel leaders and trainers. COI/T.20/Doc. No.14/Rev. 8. https://www.internationaloliveoil.org/wp-content/uploads/2023/12/COI-T.20-Doc-14-REV-8_ENK.pdf (latest access, 22th December, 2023).

Corti, F., Zanoni, B., Parenti, A., Masella, P., Breschi, C., Angeloni, G., Spadi, A., Guerrini, L., 2023. A methodological approach to estimate the overall heat transfer coefficient in olive paste malaxers. J. Food Eng. 343, 111377 https://doi.org/10.1016/j.jfoodeng.2022.111377.

Dickinson, J.R., Salgado, L.E., Hewlins, M.J., 2003. The catabolism of amino acids to long chain and complex alcohols in Saccharomyces cerevisiae. J. Biol. Chem. 278, 8028–8034. https://doi.org/10.1074/jbc.M211914200.

European Parliament and the Council (EC). Commission Delegated Regulation (EU) No 2022/2104 of 29 July 2022 supplementing Regulation (EU) No 1308/2013 of the European Parliament and of the Council as regards marketing standards for olive oil, and repealing Commission Regulation (EEC) No 2568/1991 and Commission Implementing Regulation (EU) No 29/2012.

European Parliament and the Council (EC). Commission Implementing Regulation (EU) No 2022/2105 of 29 July 2022 laying down rules on conformity checks of marketing standards for olive oil and methods of analysis of the characteristics of olive oil.

Fortini, M., Migliorini, M., Cherubini, C., Cecchi, L., Calamai, L., 2017. Multiple internal standard normalization for improving HS-SPME-GC-MS quantitation in virgin olive oil volatile organic compounds (VOO-VOCs) profile. Talanta 165, 641–652. https://doi.org/10.1016/j.talanta.2016.12.082.

Frankel, E.N., 1991. Review. Recent advances in lipid oxidation. J. Sci. Food Agric. 54 (4), 495–511. https://doi.org/10.1002/jsfa.2740540402.

García-Rodríguez, R., Romero-Segura, C., Sanz, C., Sanchez-Ortiz, A., Perez, A.G., 2011. Role of polyphenol oxidase and peroxidase in shaping the phenolic profile of virgin olive oil. Food Res. Int. 44, 629–635. https://doi.org/10.1016/j.foodres.2010.12.023.

Giannetti, V., Boccacci, Mariani, M., Colicchia, S., 2021. Furosine as marker of quality in dried durum wheat pasta: impact of heat treatment on food quality and security – a review. Food Control 125, 108306. https://doi.org/10.1016/j.foodcont.2021.108036.

Guerrini, L., Masella, P., Angeloni, G., Zanoni, B., Breschi, C., Calamai, L., Parenti, A., 2019. The effect of an increase in paste temperature between malaxation and centrifugation on olive oil quality and yield: preliminary results. Ital. J. Food Sci. 31 (3), 451–458. https://doi.org/10.14674/IJFS-1393.

Guerrini, L., Breschi, C., Zanoni, B., Calamai, L., Angeloni, G., Masella, P., Parenti, A., 2020. Filtration scheduling: quality changes in freshly produced virgin olive oil. Foods 9 (8), 1067. https://doi.org/10.3390/foods9081067.

Gutiérrez-Rosales, F., Rios, J.J., Gòmez-Rey, L., 2003. Main polyphenols in the bitter taste of virgin olive oil. Structural confirmation by on-line high-performance liquid chromatography electrospray ionization mass spectrometry. J. Agric. Food Chem. 51, 6021–6025. https://doi.org/10.1021/jf021199x.

Innocenti, M., La Marca, G., Malvagia, S., Giaccherini, C., Vincieri, F.F., Mulinacci, N., 2006. Electrospray ionisation tandem mass spectrometric investigation of phenylpropanoids and secoiridoids from solid olive residue. Rapid Commun. Mass Spectrom. 20, 2013–2022. https://doi.org/10.1002/rcm.2556.

Kalua, C.M., Bedgood jr, D.R., Bishop, A.G., Prenzler, P.D., 2006. Changes in volatile and phenolic compounds with malaxation time and temperature during virgin olive oil production. J. Agric. Food Chem. 54 (20), 7641–7651. https://doi.org/10.1021/jf061122z.

Klen, T.J., Vodopivec, B.M., 2012. The fate of olive fruit phenols during commercial olive oil processing: traditional press versus continuous two- and three-phase centrifuge. LWT - Food Sci. Technol. 49, 267–274. https://doi.org/10.1016/j.lwt.2012.03.029.

Klen, T.J., Wondra, A.G., Vrhovsek, U., Vodopivec, B.M., 2015. Phenolic profiling of olives and olive oil process-derived matrices using UPLC-DAD-ESI-QTOF-HRMS analysis. J. Agric. Food Chem. 63 (15), 3859–3872. https://doi.org/10.1021/jf506345q.

Lukic, I., Zanetic, M., Jukic Spika, M., Lukic, M., Koprivnjak, O., Brkic Bubola, K., 2017. Complex interactive effects of ripening degree, malaxation duration and temperature on Oblica cv. Virgin olive oil phenols, volatiles and sensory quality. Food Chem. 232, 610–620. https://doi.org/10.1016/j.foodchem.2017.04.047.

Lukic, I., Krapac, M., Horvat, I., Godena, S., Kosic, U., Brkic Bubola, K., 2018. Three-factor approach for balancing the concentrations of phenols and volatiles in virgin olive oil from a late-ripening olive cultivar. LWT – Food Sci. Technol. 87, 194–202. https://doi.org/10.1016/j.lwt.2017.08.082.

Miho, H., Moral, J., Lopez-Gonzalez, M.A., Diez, C.M., Priego-Capote, F., 2020. The phenolic profile of virgin olive oil is influenced by malaxation conditions and determines the oxidative stability, 126183 Food Chem. 314. https://doi.org/10.1016/j.foodchem.2020.126183.

Morales, M.T., Luna, G., Aparicio, R., 2005. Comparative study of virgin olive oil sensory defects. Food Chem. 91, 293–301. https://doi.org/10.1016/j.foodchem.2004.06.011.

Nardella, M., Moscetti, R., Bedini, G., Bandiera, A., Chakravartula, S.S.N., Massantini, R., 2023. Impact of traditional and innovative malaxation techniques and technologies on nutritional and sensory quality of virgin olive oil – a review, 100163 Food Chem. Adv. 2. https://doi.org/10.1016/j.focha.2022.100163.

Nursten, H., 2005. The Maillard reaction. Chemistry, biochemistry ad implications. By Harry Nursten. The Royal Society of Chemistry (London, UK).

Rodgers, S., 2016. Minimally processed functional foods: technological and operational pathways. J. Food Sci. 81 (10), R2309–R2319. https://doi.org/10.1111/1750-3841.13422.

Ryan, D., Antolovich, M., Prenzler, P., Robards, K., Lavee, S., 2002. Biotransformations of phenolic compounds in *Olea europaea* L. Sci. Hortic. 92 (2), 147–176. https://doi.org/10.1016/S0304-4238(01)00287-4.

Sharma, R., Prakash, O., Sonawane, M.S., Nimonkar, Y., Golellu, B.P., Sharma, R., 2016. Diversity and distribution of phenol oxidase producing fungi from Soda Lake and description of Curvularia lonarensis sp. nov. Front. Microbiol. 7, 1847. https://doi.org/10.3389/fmicb.2016.01847.

Toydemir, G., Subasi, B.G., Hall, R.D., Beekwilder, J., Boyaciuglu, D., Capanoglu, E., 2022. Effect of food processing on antioxidants, their bioavailability and potential relevance to human health. Food Chem: X 14, 100334. https://doi.org/10.1016/j.fochx.2022.100334.

Trapani, S., Breschi, C., Cecchi, L., Guerrini, L., Mulinacci, N., Parenti, A., Canuti, V., Picchi, M., Caruso, G., Gucci, R., Zanoni, B., 2017a. Indirect indices of oxidative damage to phenolic compounds for the implementation of olive paste malaxation optimization charts. J. Food Eng. 207, 24–34. https://doi.org/10.1016/j.jfoodeng.2017.03.012.

Trapani, S., Guerrini, L., Masella, P., Parenti, A., Canuti, V., Picchi, M., Caruso, G., Gucci, R., Zanoni, B., 2017b. A kinetic approach to predict the potential effect of malaxation time-temperature conditions on extra virgin olive oil extraction yield. J. Food Eng. 195, 182–190. https://doi.org/10.1016/j.jfoodeng.2016.09.032.

Vichi, S., Romero, A., Gallardo-Chacon, J., Tous, J., Lopez-Tamames, E., Buxaderas, S., 2009. Influence of Olives' storage conditions on the formation of volatile phenols and their role in off-odor formation in the oil. J. Agric. Food Chem. 57, 1449–1455. https://doi.org/10.1021/jf803242z.

Zanoni, B., 2014. Which processing markers are recommended for measuring and monitoring the transformation pathways of main components of olive oil? Ital. J. Food Sci. 26 (1), 3–11.

Zhu, H., Wang, S.C., Shoemaker, C.F., 2016. Volatile constituents in sensory defective virgin olive oils. Flavour Fragr. J. 31, 22–30. https://doi.org/10.1002/ffj.3264.

Zullo, B.A., Ciafardini, G., 2022. Role of yeasts in the qualitative structuring of extra virgin olive oil. J. Appl. Microbiol. 132 (6), 4033–4041. https://doi.org/10.1111/jam.15478.